Supporting Information

Boosting oxygen electrocatalytic reactions with Mn_3O_4/self-growth N-doped carbon nanotubes induced by transition metal cobalt

Li-Na Lu [a], Cheng Chen [a], Kang Xiao [a], Ting Ouyang [a], Jun Zhang*[b], Zhao-Qing Liu*[a]

[a]School of Chemistry and Chemical Engineering/Institute of Clean Energy and Materials/Guangzhou Key Laboratory for Clean Energy and Materials, Guangzhou University, Guangzhou Higher Education Mega Center, No. 230 Wai Huan Xi Road, 510006, P. R. China. E-mail: lzqgzu@gzhu.edu.cn (Z. Q. Liu)

[b]State Key Laboratory of Advanced Technology for Material Synthesis and Processing, Wuhan University of Technology, Luoshi Road 122#, Wuhan 430070, P.R. China. E-mail: zj2011@whut.edu.cn (J. Zhang)

Contents

1. Experimental Section

2. Supplementary Figures

1. Experimental Section

1.1 Preparation Methods

All reagents and raw materials used in this work are analytical grade and without further purification. $Co(NO_3)_2·6H_2O$ (98%, AR) was obtained from Guangzhou Chemical Reagent Factory, Melamine (99.5%, AR) and glucose (99%, AR) were gained from Tianjin Damao Chemical Reagent Factory and Tianjin Fuchen Chemical Reagent Factory respectively, $KMnO_4$ (99.5%, AR) was purchased from Tianjin HongDa Chemical Reagent Factory. Commercial Pt/C (Pt 20 wt.%) was bought from Shanghai Hesen Electric Co. Ltd. commercial IrO_2 (IrO_2 85%, Ar) was gained from Shanghai Hansi Chemical Industry Co. Ltd.

1.2 Synthesis of catalysts

1.2.1 Synthesis of NCNTs/Co

As a carbon carrier, NCNTs/Co was synthesized by a simple method of vapor deposition. 0.10 g $Co(NO_3)_2·6H_2O$, 0.05 g glucose and 4.00 g melamine are grinding evenly. Then the hybrid precursor was transferred into a porcelain boat and annealed in Ar atmosphere at 800 °C for 2 h (the heating rate is 2 °C min^{-1}).

1.2.2 Synthesis of Mn_3O_4/NCNTs/Co

Mn_3O_4/NCNTs/Co were synthesized by means of a simple one pan procedure, the Mn_3O_4 nanoparticles were grown evenly on the surface of NCNTs/Co. First, 0.02 g, 0.03 g and 0.04g $KMnO_4$ were placed in a clean beaker, respectively, and then 0.03 g NCNTs/Co and 30 mL distilled water were added in each beaker. second, the solution in the beaker by continuous ultrasonication for 15 min was transferred to a 50 mL reaction kettle for

hydrothermal reaction at 160 °C for 9 h. After the reaction kettle cooled to room temperature, the target product was collected by multiple centrifugation using water, and dried at 60℃ for 6 h. The obtained product was labeled as Mn_3O_4/NCNTs/Co-1, Mn_3O_4/NCNTs/Co-2 and Mn_3O_4/NCNTs/Co-3 in turn. Except for not adding NCNTs/Co, the Mn_3O_4 was obtained follow the same synthesis steps of Mn_3O_4/NCNTs/Co-3.

1.3 Physicochemical Characterizations

Sample morphologies were characterized using Transmission electron microscopy (TEM, 300 kV, Tecnai™ G2 F30) and Field emission scanning electron microscope (SEM, JEOL JSM-7600F). The crystalline phases information of the as-prepared samples was collected by X-ray diffraction (XRD) patterns with Cu Kα radiation source, XRD was operated at 40 kV and 120 mA in a 2θ angular range of 5−80°. Detailed element composition and chemical state of samples was collected by X-ray photoelectron spectroscopy (XPS, ESCALAB 250Xi instrument). Using 514-nm laser, The Raman spectra were acquired on a Raman spectrometer (JY, HR 800).

1.4 Electrochemical measurements

1.4.1 Electrode preparation

Under identical conditions with the same catalyst mass loading, the ORR and OER electrochemical analysis were performed. The 4.0 mg as-synthesized catalyst was dissolved in the mixture solution (0.3 mL distilled water, 0.7 mL ethanol, and 20 μL Nafion® solution), then sonication for 30 min to get catalyst ink. Followed by 8 μL of the catalyst ink was transferred onto glassy carbon rotating ring disk electrode (RRDE, 0.196 cm^{-2}) and dried in air, the catalyst loading on RRDE is 0.18 mg cm^{-2}.

1.4.2 Electrochemical testing

Other electrochemical tests were conducted at a three-electrode cell with the Princeton electrochemical workstation, except for the performance of Zinc-air batteries was performed in an electrochemical workstation (CHI600e). A standard three-electrode system, a platinum foil, and a rotating ring disk electrode (RRDE) with a glassy-carbon electrode (area 0.196 cm^2) were employed as reference, counter, and working electrodes, respectively. All potentials in this study are converted to RHE according to the Nernst equation, where E_{RHE} (V) = E_{SCE} + 0.244 + 0.059 × pH.

The OER polarization curves with sweep rate of 10 mV s^{-1} were recorded at 1600 rotational speeds in 1_M KOH solution. The ORR polarization curves with sweep rate of 10 mV s^{-1} at different rotational speeds were gained in oxygen saturated 0.1 $_M$ KOH solution, and the rotational speeds were from 400 to 2025 rpm.

The electron transfer number (*n*) was calculated by koutech-Levich (K-L) equation:

$$J^{-1} = J_k^{-1} + (B\omega^{1/2})^{-1} \quad (1)$$

$$B = 0.62(D_0)^{2/3}v^{-1/6}C_0 \quad (2)$$

$$J_k = nFkC_0 \quad (3)$$

where *J* represents the measured current density, J_k is kinetic current density, B and ω are slope of K-L plots and electrode rotating angular velocity, respectively. v means the kinetic viscosity (0.01 $cm^2\ s^{-1}$), as well as C_0 represents the bulk concentration of O_2 (1.2 × 10^{-3} mol L^{-1}). F is the Faraday constant (96485 $C\ mol^{-1}$), D_0 is the diffusion coefficient of O_2 (1.9 × 10^{-5} $cm^2\ s^{-1}$), *n* means the electron transfer number.

The mean electron transfer number (*n*) and H_2O_2 yield of the ORR also can been

estimated by the RRDE method according to equation (4), (5):

$$n = \frac{4J_D}{J_D + (J_R/N)} \quad (4)$$

$$H_2O_2\% = 100\frac{2(J_R/N)}{J_D + (J_R/N)} \quad (5)$$

Where n represent the mean electron transfer number of the ORR. J_D, J_R and N represent the disk current, ring current and the collection efficiency of the RRDE (37 %), respectively.

CV measurements are conducted with the varying scan rates from 5 to 30 mV s^{-1} by sweeping the potential across the non-Faradaic region. The measured current density in this non-Faradaic potential region is mainly caused by a double layer charge. the electrochemical active surface area (ECSA) was gained by the equation (6):

$$ECSA = C_{dl}/C_s \quad (6)$$

where C_s is the specific capacitanc. Electrochemical impedance spectroscopy (EIS) was collected from 1 Hz to 100 KHz at open-circuit potential (OCP). When chronoamperometry at 0.4 V, the stability of ORR was characterized.

1.4.3 Zn-air Battery Assembly

The rechargeable *Zn-air Battery* were tested in a home-made electrochemical cell using 6 M KOH solution as the liquid electrolyte, Zinc foil was used as anode and catalysts loaded on the gas diffusion layer (Nafion-coated carbon fiber paper with a geometric area of 1.21 cm^2, catalyst loading amount of 7.0 mg cm^{-2}) was acting as the air cathode. All

data of the as-fabricated cell were tested on CHI760E electrochemical workstation at room temperature. For comparison, the air cathode was consisted of the coupled noble metal Pt/C (Pt/C: IrO_2 mass ratio is 1:1) catalyst.

2. Supplementary Figures

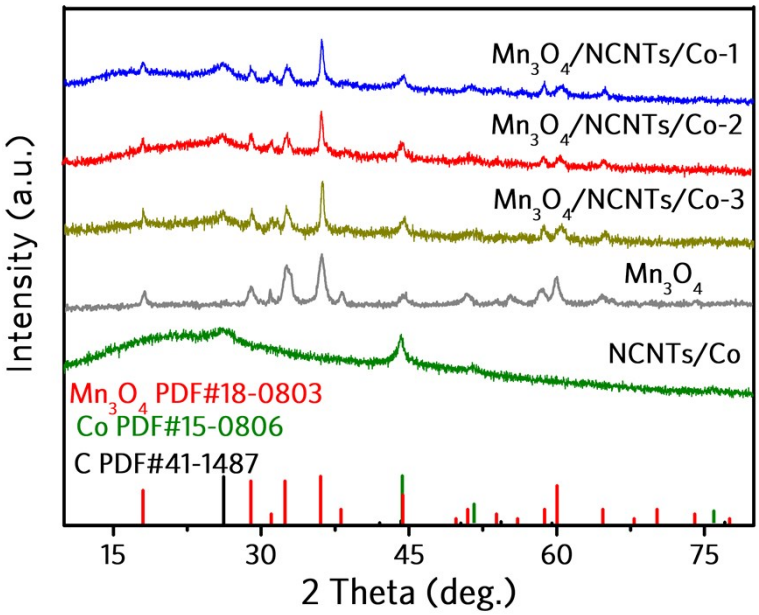

Fig S1. XRD of Mn_3O_4/NCNTs/Co-1, Mn_3O_4/NCNTs/Co-2, Mn_3O_4/NCNTs/Co-3, Mn_3O_4 and NCNTs/Co samples.

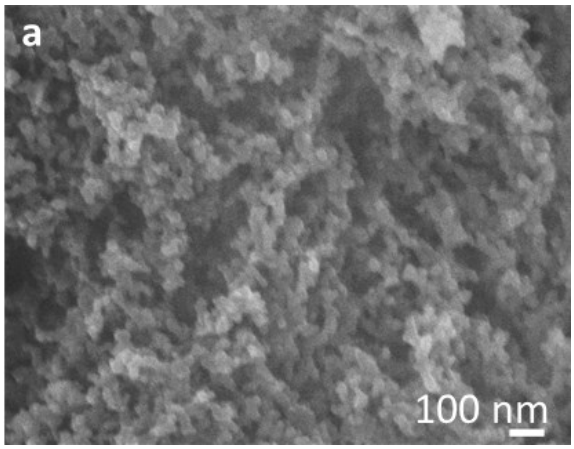

Fig S2. SEM of a) Mn_3O_4.

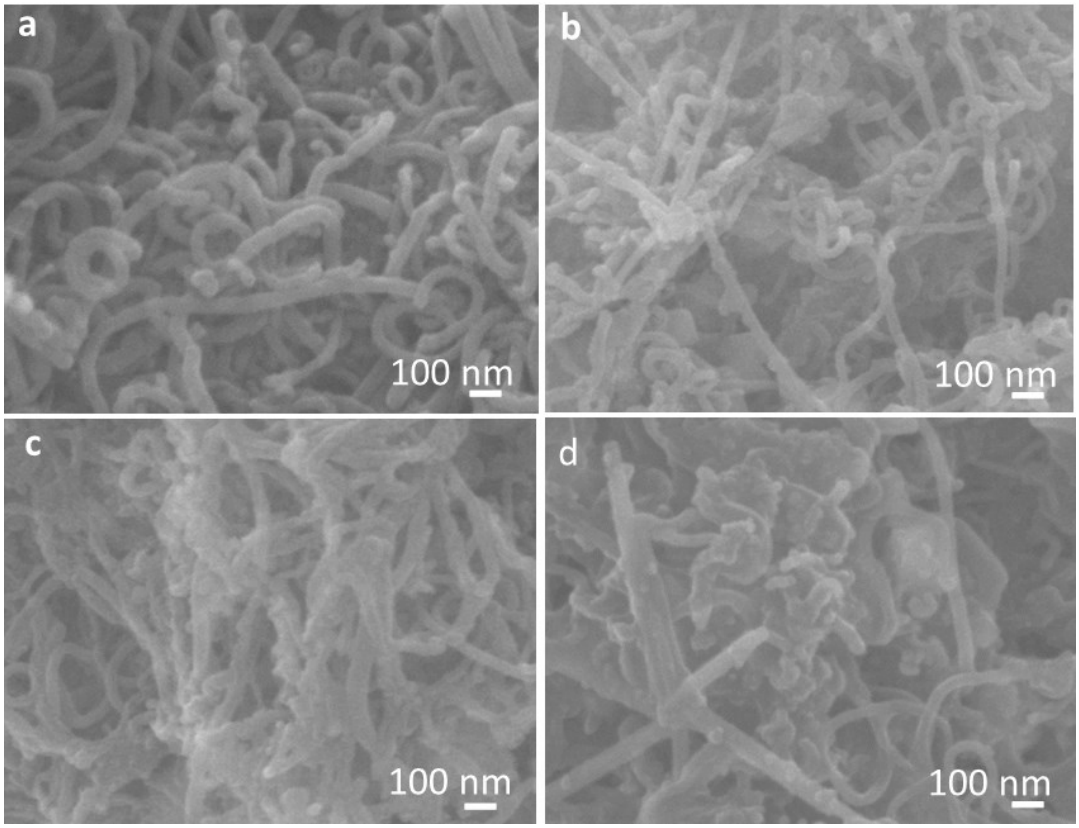

Fig S3. SEM of a) NCNTs/Co, b) Mn_3O_4/NCNTs/Co-1, c) Mn_3O_4/NCNTs/Co-2 and d) Mn_3O_4/NCNTs/Co-3.

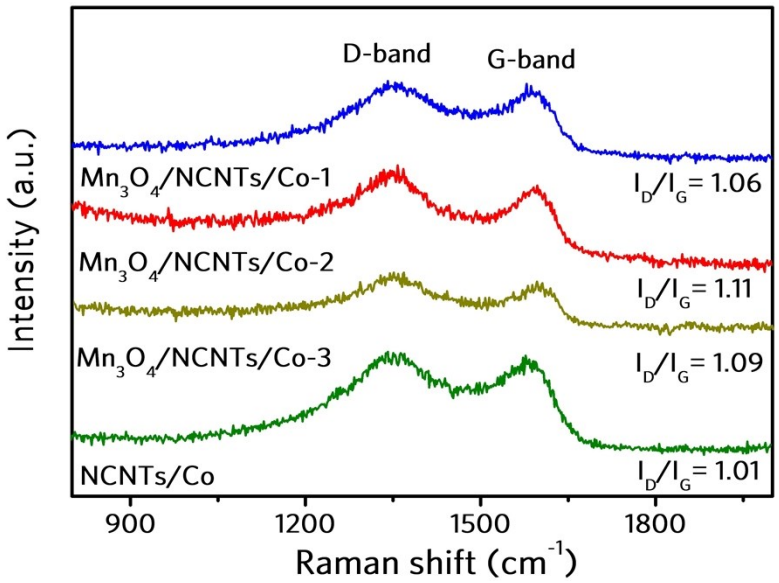

Fig S4. Raman spectra of NCNTs/Co, Mn_3O_4/NCNTs/Co-1, Mn_3O_4/NCNTs/Co-2 and Mn_3O_4/NCNTs/Co-3 samples.

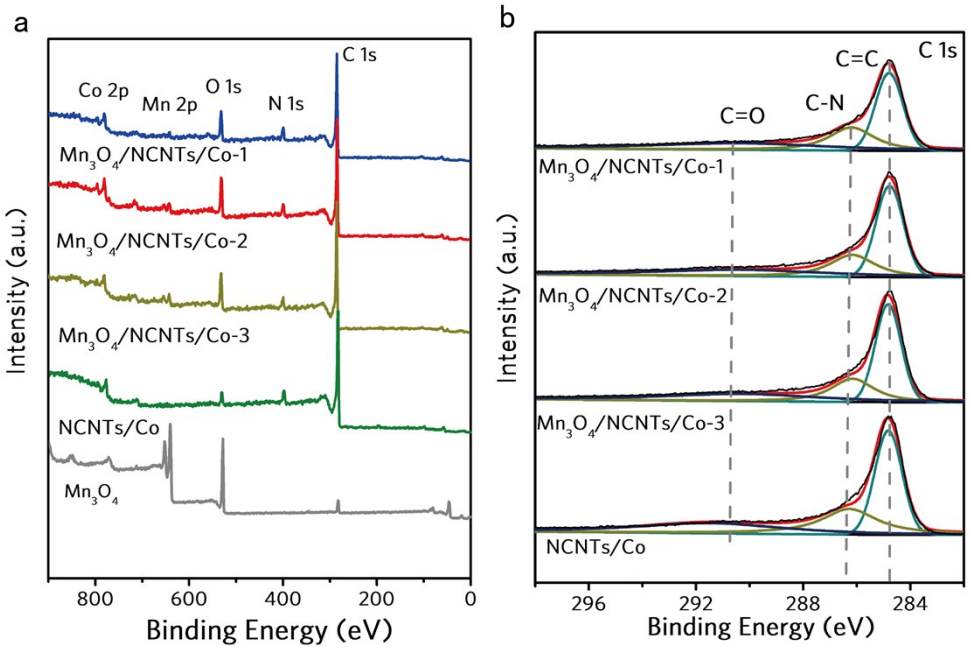

Fig S5. High-resolution a) survey, b) C 1s XPS spectra of NCNTs/Co, Mn_3O_4/NCNTs/Co-1, Mn_3O_4/NCNTs/Co-2, Mn_3O_4/NCNTs/Co-3.

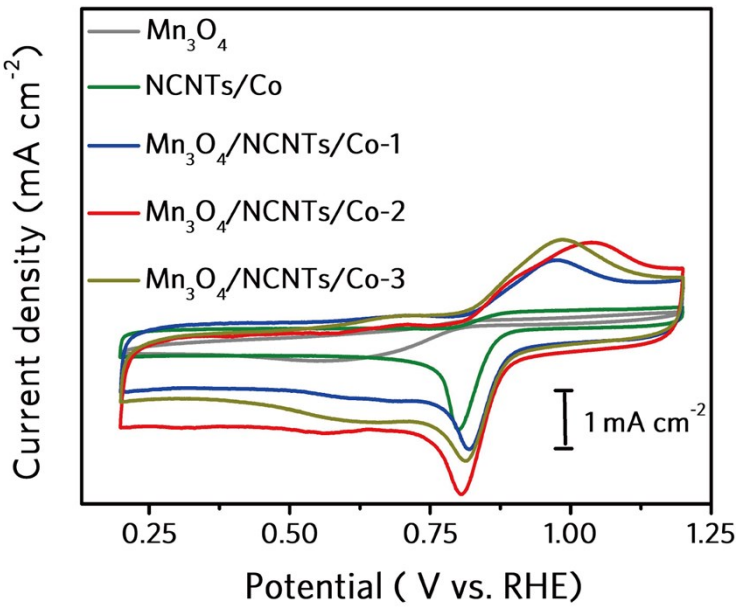

Fig S6. CV curves of Mn_3O_4, NCNTs/Co, Mn_3O_4/NCNTs/Co-1, Mn_3O_4/NCNTs/Co-2, Mn_3O_4/NCNTs/Co-3 in an O_2-saturated 0.1 M KOH solution at the scan rate of 50 mV s^{-1}.

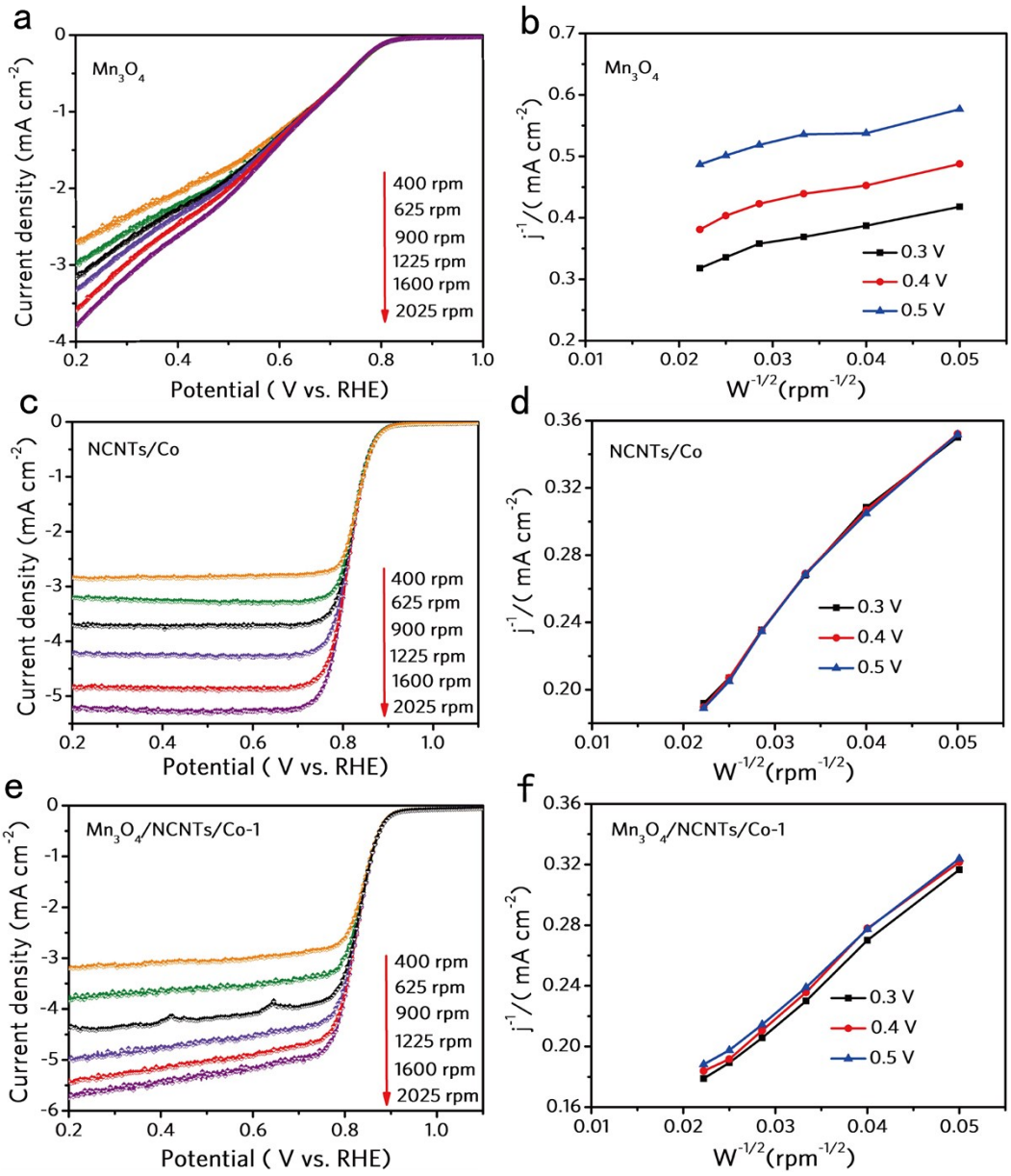

Fig S7. LSVs with different scanning rates (400 to 2025 rpm) and the corresponding Koutecky-Levich plots at different potentials of a) and b) Mn_3O_4, c) and d) NCNTs/Co, e) and f) Mn_3O_4/NCNTs/Co-1.

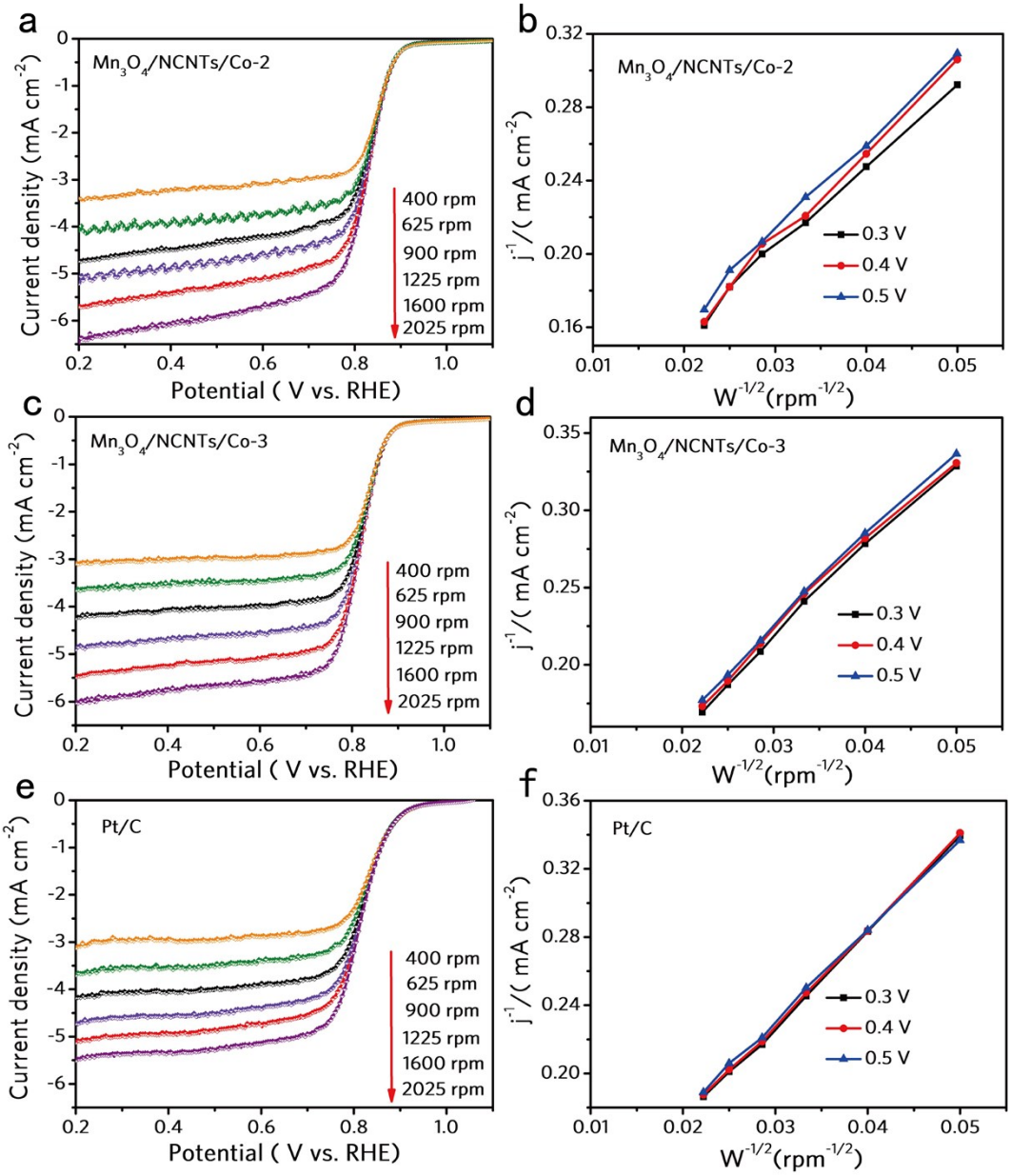

Fig S8. LSVs with different scanning rates (400 to 2025 rpm) and the corresponding Koutecky-Levich plots at different potentials of a) and b) Mn_3O_4/NCNTs/Co-2, c) and d) Mn_3O_4/NCNTs/Co-3, e) and f) Pt/C.

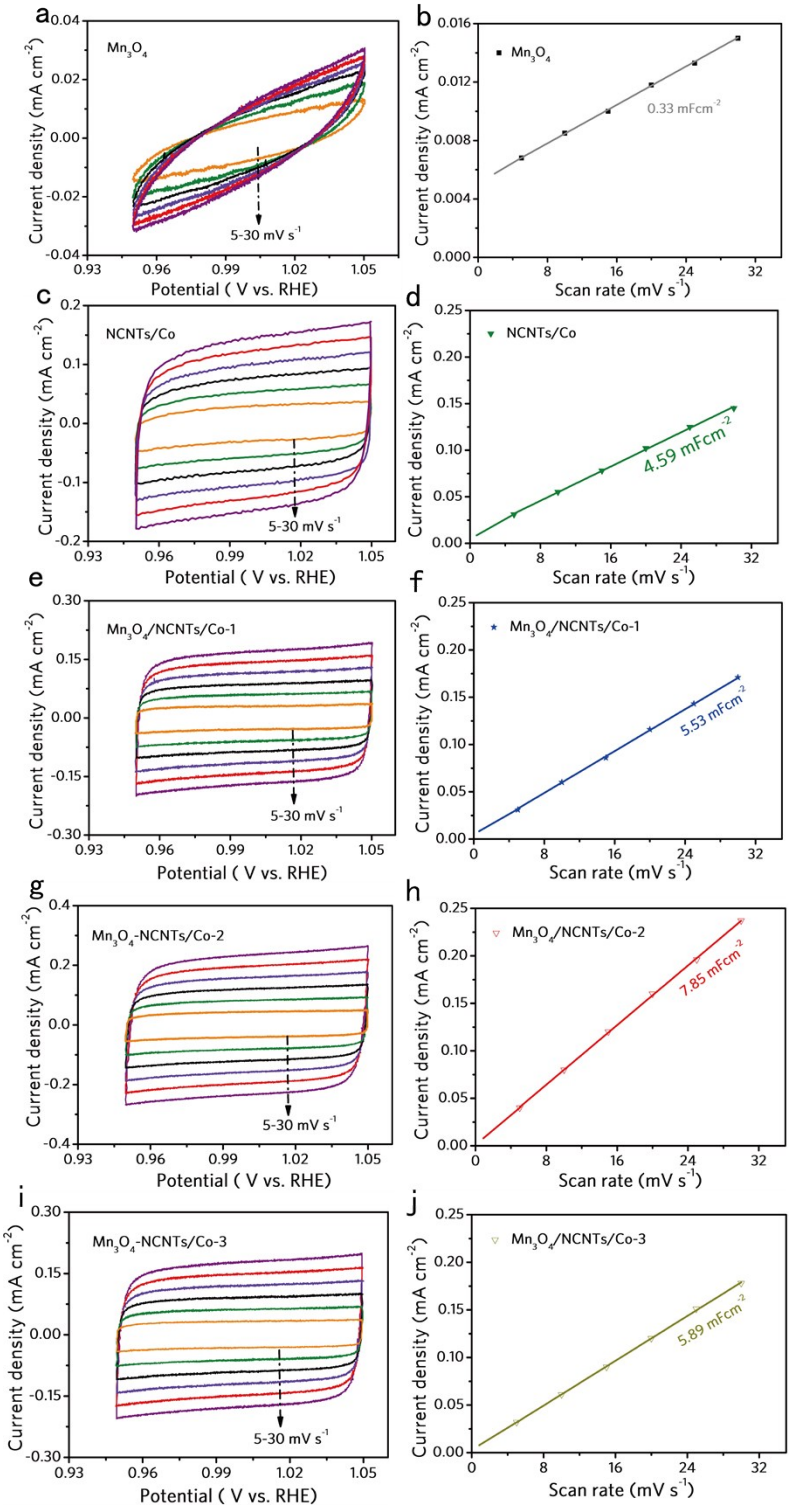

Fig S9. The CVs measured at different scan rates and the electrical double-layer capacitor of a) and b) Mn_3O_4, c) and d) NCNTs/Co, e) and f) Mn_3O_4/NCNTs/Co-1, g) and h) Mn_3O_4/NCNTs/Co-2, i) and j) Mn_3O_4/NCNTs/Co-3.

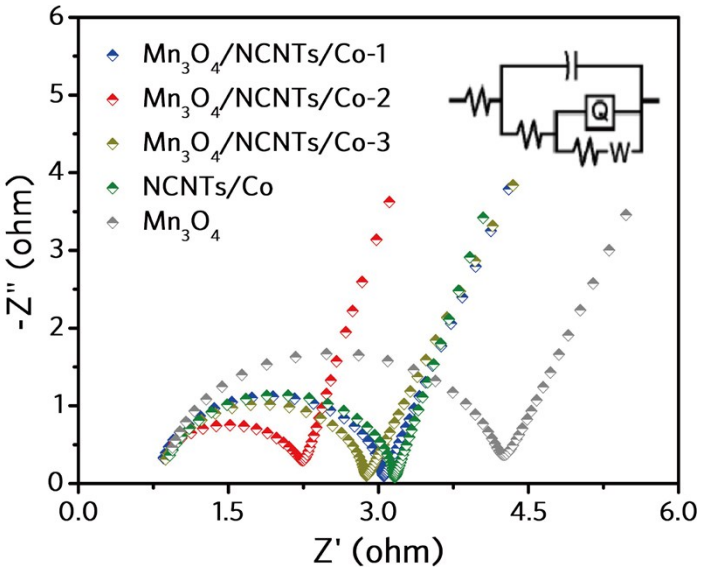

Fig S10. Nyquist plots, inset: the equivalent circuit diagram.

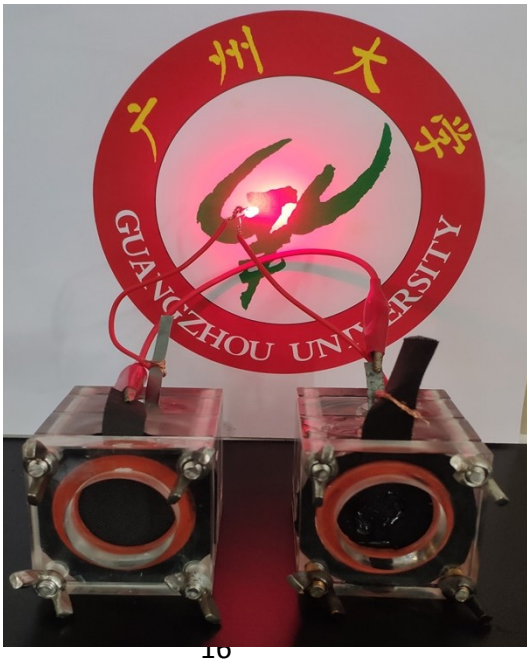

Fig S11. Red LED (1.8 V) photos powered in series by two sets of homemade batteries.

Table S1. Element content of C, O, N, Co and Mn in different catalysts calculated by XPS scan.

Catalyst	Element content (At.%)				
	C	O	N	Co	Mn
NCNTs/Co	90.10	3.26	5.48	1.17	-
Mn_3O_4/NCNTs/Co-1	88.17	8.96	1.12	1.18	0.57
Mn_3O_4/NCNTs/Co-2	81.88	10.43	5.02	1.66	1.01
Mn_3O_4/NCNTs/Co-3	82.15	10.08	5.13	1.63	1.01

Table S2. The ORR and OER activities of as-prepared catalysts in this work.

	Mn_3O_4/NCNTs/Co-2	NCNTs/Co	Pt/C	IrO_2
Catalyst Loading (mg cm^{-2})	0.18	0.18	0.18	0.18
ORR part				
$E_{1/2}$ (V vs.RHE)	0.83	0.81	0.81	
j at E = 0.2V (mA cm^{-2})	-5.7	-4.8	-5.1	
Onset potential (V vs.RHE)	0.94	0.91	0.98	
Tafel slope (mV dec^{-1})	56	67	83	
OER part				
η_{10} (mV)	390	450		350
Onset potential (V vs.RHE)	1.55	1.59		1.50
Tafel slope (mV dec^{-1})	104	134		99

Table S3. Comparison for ORR activity in 0.1 M KOH for Mn_3O_4/NCNTs/Co-2 with other recently reported electrocatalysts.

Catalyst	Current density	Tafel slope	$E_{1/2}$ (V)	n	Ref.
Mn_3O_4/NCNTs/Co-2	-5.7	56	0.83	3.75	This work
NCNTs/Co	-4.8	67	0.81	3.45	This work
Pt/C	-5.1	83	0.81	3.95	This work
FeCo-DHO/NCNTs	-6.4	36	0.86	-	*Adv. Energy Mater*, *2018*, **8**, 1801836
CoO/hi-Mn_3O_4	-2.9	-	-	3.8	*Angew. Chem. Int. Ed*, 2017, **56**, 8539-8543
Co/CoOx@BS-NCNTs-700	-5.8	56	0.84	3.9	*J Colloid Interface Sci*, 2019, **557**, 580-590
Mn_3O_4/O-CNT	-3.26	-	0.85	3.95	*ACS Appl. Energy Mater,* 2018, **1**, 963-969.
a-MnO_x/TiC	-5.5	72	0.80	3.90	*Nano Energy*, 2020, **67**, 104208
MnO/NC-2	-5.4	58	0.88	-	*Chem. Eur. J*, 2019, **25**, 2868-2876
C-MnO_2	-3.4	-	0.75	3.84	*ACS Appl. Mater. Interfaces,* 2018, **10**, 2040-2050.

Table S4. Comparison for OER activity in 1 M KOH for Mn_3O_4/NCNTs/Co-2 with other recently reported electrocatalysts.

Catalyst	η_{10} @OER	Tafel slope	Ref.
Mn_3O_4/NCNTs/Co-2	390	104	This work
NCNTs/Co	450	132	This work
IrO_2	350	99	This work
CoO/hi-Mn_3O_4	378	61	*Angew. Chem. Int. Ed,* 2017, **56**, 8539-8543
Co/CoOx@BS-NCNTs-700	360	112	*J Colloid Interface Sci,* 2019, **557**, 580-590
Mn_3O_4/O-CNT	410	75	*ACS Appl. Energy Mater,* **2018,** *1*, 963-969.
Co/β-Mo_2C@N-CNTs	356	67	*Angew. Chem. Int. Ed,* 2019, ***58***, 4923-4928.
Doped MnO_2/CFP	390	104.4	*Adv. Funct. Mater,* 2017, **27**, 1701833
Co/MnO_2	400	60	*J. Phys. Chem. C,* 2018, **122**, 8406-8413